Biomaterials Science

PAPER

View Article Online
View Journal | View Issue

Cite this: *Biomater. Sci.*, 2014, **2**, 98

Biologically inspired membrane design with a heparin-like interface: prolonged blood coagulation, inhibited complement activation, and bio-artificial liver related cell proliferation†

Shengqiang Nie,‡[a,b] Min Tang,‡[a,b] Chong (Sage) Cheng,*[a,b] Zehua Yin,[a,b] Lingren Wang,[a,b] Shudong Sun[a,b] and Changsheng Zhao*[a,b]

In the present work, inspired by the chemical structure of heparin molecules, we designed a polyethersulfone (PES) membrane with a heparin-like surface for the first time by physically blending sulfonated polyethersulfone (SPES), carboxylic polyethersulfone (CPES), and PES at rational ratios. Evaporation and phase-inversion membranes of PES/CPES/SPES were prepared by evaporating the solvent in a vacuum oven, and by a liquid–liquid phase separation technique, respectively. Scanning electron microscopy (SEM) images revealed that the structures of the PES/CPES/SPES membranes were dependent on the proportions of the additives and no obvious phase separation was detected. The blood compatibility of the modified membrane surfaces was characterized in terms of bovine serum fibrinogen (BFG) adsorption, platelet adhesion, thrombin–antithrombin (TAT) generation, percentage of platelets positive for CD62p expression, clotting times (activated partial thromboplastin time (APTT) and prothrombin time (PT)), and complement activation on C3a and C5a levels. The results indicated that the blood compatibility of PES matrix was improved due to the biologically inspired membrane design with a heparin-like interface by introducing functional sulfonic acid and carboxylic acid groups. Furthermore, cell morphology observation and cell culture assays demonstrated that the modified membranes showed better performance in bio-artificial liver related cell proliferation than the pristine PES membrane. In general, the intriguing PES/CPES/SPES membranes, especially the phase-inversion one, showed improved blood and cell compatibility, which might have great potential application in the blood purification field.

Received 2nd July 2013,
Accepted 8th August 2013

DOI: 10.1039/c3bm60165j

www.rsc.org/biomaterialsscience

1. Introduction

With the development of modern medicine, artificial materials are widely applied in the biomedical field during hemodialysis, cardiopulmonary by-pass, and other procedures that require disposable clinical instruments. Excellent biocompatibility is the essential and highly pursued character for the design of advanced artificial devices used to substitute for or operate in contact with blood, live tissues and organs. Among various evaluation indices, blood compatibility has been considered to be the most essential part of biocompatibility for blood-contact devices. The formation of a thrombus can be aggravated when blood proteins are adsorbed onto the material, which can cause artery occlusion. The reduction in blood supply caused by thrombosis can result in severe injury, including heart attack, and even death.[1] Thus, blood compatibility has been extensively evaluated to avoid thrombosis and other material-related adverse events in the hematic environment.[2]

Among the materials used in the blood-contact field, polyethersulfone (PES) and PES-based materials, which have good oxidative, thermal, and hydrolytic stabilities, as well as good mechanical and film-forming properties, have been widely applied in the fields of artificial organs and medical devices used for blood purification.[3–8] However, as a blood-contact material, the blood compatibility of pristine PES membrane is not adequate and its application in blood-contacting devices is greatly limited, *e.g.* hemodialysis and artificial organs.[9,10] Thus, the blood compatibility of PES should be improved to adapt to the hematic environment when it is used as a blood-

[a]*College of Polymer Science and Engineering, State Key Laboratory of Polymer Materials Engineering, Sichuan University, Chengdu 610065, People's Republic of China. E-mail: sagecheng@163.com, zhaochsh70@163.com, zhaochsh70@scu.edu.cn; Fax: +86-28-85405402; Tel: +86-28-85400453*
[b]*National Engineering Research Center for Biomaterials, Sichuan University, Chengdu 610l064, People's Republic of China*

† Electronic supplementary information (ESI) available: UV-Vis spectra, heparin inspired interface design and activation of red cells and platelets, CD62p-positive platelet expression. See DOI: 10.1039/c3bm60165j

‡ These two authors contributed equally to this work.

contact material. With respect to the hydrophilicity and blood compatibility of PES,[11] modifications have been reported in many previous efforts. The modification techniques for PES membranes generally include blending, surface assembly and coating, surface physical treatment, and surface grafting.[12–18] For the improvement of blood compatibility of PES membranes, one of the key events is finding materials with good blood compatibility to modify the PES matrix.

Heparin, which is composed primarily of sulphated disaccharides, is the most commonly used anticoagulant in haemodialysis and the most widely applied biopolymer in surface modification.[19] A number of studies suggested that the heparin grafted surfaces showed a diminished thrombogenic response.[20,21] Nevertheless, with the long-term usage of heparinized materials, the dramatic loss of bioactivity and degradation *in vivo* may occur due to covalent or noncovalent binding with blood components.[22] Moreover, these methods also suffer from some inherent drawbacks, *e.g.*, some hazardous reagents are used in the grafting process, which are difficult to remove completely and may contaminate the obtained materials, and many of these methods are complicated and require additional steps in the preparation process, which may restrict the application of heparin-immobilized materials.[23–26]

Inspired by the biological blood and cell compatibility of heparin, we have produced many efforts to design heparin-like macromolecules to improve the biocompatibility of PES membranes by mimicking the structure of heparin *via* the introduction of the functional groups, such as sulfonic acid group or carboxylic acid group containing polymers.[27–30] Through a facile physical blending approach, these functional heparin-like macromolecules have been used for improving the blood compatibility of PES membranes. In previous studies,[27–29] the prepared heparin-like PES membranes have revealed good blood compatibility with inhibited platelet adhesion and activation, prolonged clotting time, *etc.* However, the amount of polymer blended into the PES matrix was limited due to poor miscibility between the polymers and PES.

In the present work, inspired by the chemical structure of heparin, we design a PES membrane with a heparin-like surface for the first time by blending sulfonated polyethersulfone (SPES), carboxylic polyethersulfone (CPES), and PES at different ratios. To assess the performance of the prepared PES/CPES/SPES membrane in detail, two of the most common approaches for membrane fabrication are taken; evaporation and phase-inversion membranes of PES/CPES/SPES were prepared by evaporating the solvent in a vacuum oven, and by a liquid–liquid phase separation technique, respectively. Scanning electron microscopy (SEM) images revealed that the structures of the PES membranes were dependent on the proportions of the additives, and the blending system exhibited good miscibility and no obvious phase separation was observed due to the same polymer backbone of SPES, CPES and PES. ATR-FTIR and XPS tests were used to confirm the surface aggregation of these heparin-like macromolecules on the PES membrane surface. Furthermore, the effect of functional groups and preparation methods on the blood compatibility and cell proliferation was investigated by observing the following characteristics: water contact angle, protein adsorption, blood compatibility (platelet adhesion, thrombin–antithrombin (TAT) generation, platelet activation, clotting time, complement activation (C3a and C5a), and cytocompatibility (cell morphology and cell viability assays).

2. Materials and methods

2.1 Materials

Polyethersulfone (PES, Ultrason E6020P) was purchased from BASF, Germany. Chlorosulfonic acid (CSA) and dichloromethane (CH_2Cl_2, reagent grade) were purchased from Chengdu Kelong Chemical Inc. (Chengdu, China), and used without further purification. Acetyl chloride (CH_3COCl) was purchased from Tianjin Kemel Chemical Reagent Company. *N*-Methyl-2-pyrrolidone (NMP; AR, 99.0%) was purchased from Chengdu Kelong Chemical Inc. (Chengdu, China), and used as the solvent. $KMnO_4$ was purchased from Chengdu Changlian Chemical Reagent Company. Bovine serum fibrinogen (BFG) was obtained from Sigma Aldrich, USA. Micro BCA™ Protein Assay Reagent kits were the products of PIERCE. Anti-$CD62P^{PE}$ antibodies were purchased from Beckman Coulter, CA. Thrombin–antithrombin complex (TAT) (Enzygnost TAT micro) was obtained from Assay Pro, USA. C3a and C5a ELISA kits were purchased from Cusbio Biotech Co., Ltd, China. 3-(4,5-Dimethylthiazol-2-yl)-2,5-diphenyl tetrazolium bromide (MTT) was purchased from Sigma. All the other chemicals (analytical grade) were obtained from the Chengdu Kelong Inc, China, and were used without further purification.

2.2 Synthesis and characterization of SPES and CPES

SPES was prepared according to the developed method from previous work,[31,32] as shown in Scheme 1. Briefly, 10 g of PES, which had been dried in a vacuum oven at 110 °C for 1 h, was dissolved in 80 mL CH_2Cl_2. Then, chlorosulfonic acid solution (CH_2Cl_2 as the solvent, the molar ratio of chlorosulfonic acid to PES was 10 : 1) was added drop-wise to the PES solution under stirring at 16 °C for about 30 minutes, then an additional hour was taken to complete the reaction, and the whole process was under nitrogen protection to inhibit the side reaction. The mixture was then gradually precipitated into deionized water under agitation, and the resulting precipitate was obtained by filtration, washing with deionized water until the pH value of the filtrate was the same as the deionized water. Finally, the obtained SPES was dried at 30 °C in a vacuum oven for about 48 h.

Carboxylic polyethersulfone (CPES) was prepared according to our recent study,[33] as shown in Scheme 1. Briefly, PES was dissolved in NMP with a concentration of 20 wt% for the acetylating reaction. Acetyl chloride (used as an acetylating reagent) and $AlCl_3$ (used as catalyst) were mixed with NMP. The mixed solution was then poured into the PES solution slowly at a temperature of 90 °C. After 2 h, the product (PES-$COCH_3$) was

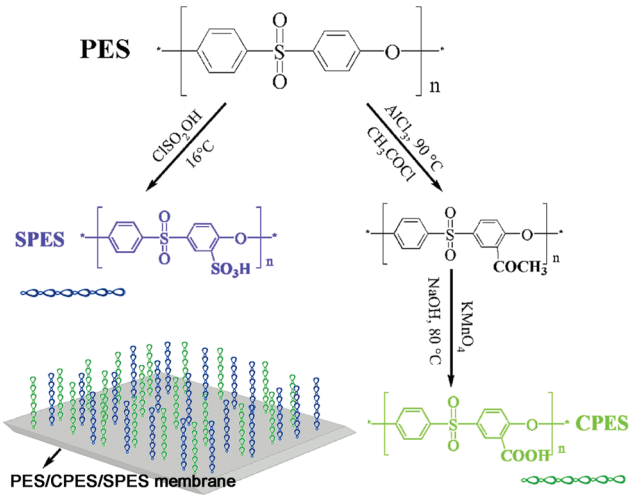

Scheme 1 Synthetic procedure for the SPES and CPES polymers. The PES/CPES/SPES composite membranes were prepared by blending SPES, CPES, and PES at different ratios with surface aggregated functional sulfonic acid and carboxylic acid polymer chains.

washed with double distilled water and dried in an oven for 24 h. In the oxidation reaction procedure, PES-$COCH_3$ was dissolved in NMP with a concentration of 20 wt%. $KMnO_4$ and NaOH were dissolved in a mixed solution of double distilled water and NMP. The mixed solution was then added into the PES-$COCH_3$ solution slowly at 80 °C with stirring. After 6 h, the product was obtained through a centrifugal process using a centrifugal machine at approximately 4000 rpm. The obtained CPES was dried in a vacuum oven for 24 h.

^{1}H-NMR spectra were recorded with a Bruker DRX 300 spectrometer (Bruker Co., Germany) to analyze SPES and CPES, using deuterated dimethyl sulfoxide (DMSO-d_6) as a solvent. FTIR analysis of the polymers was performed using a Nicolet 560 spectrometer (America). The SPES and CPES were first dried in a vacuum oven overnight at room temperature, and then ground with KBr and pressed into tablets. A pristine PES sample was also prepared.

2.3 Preparation and characterization of modified PES membranes

2.3.1. Preparation. PES modified membranes were prepared in the form of phase-inversion and evaporation membranes using a liquid–liquid phase separation technique and evaporation method, respectively.

The casting solutions were prepared as follows: PES, SPES and CPES were dissolved in NMP, and the solution was vigorously stirred until a clear homogeneous solution was obtained. The total concentration of all the polymers was 16 wt%. In the study, different kinds of membranes were prepared by changing the amounts of PES, SPES and CPES in the casting solutions, and the ratios of PES, CPES and SPES were 16 : 0 : 0, 8 : 8 : 0, 8 : 6 : 2, 8 : 4 : 4, 8 : 2 : 6, and 8 : 0 : 8.

To prepare the phase-inversion membrane, the casting solution was vacuum degassed and then prepared into membrane by a spin coating method based on a liquid–liquid phase separation method at room temperature, which produced a white-coloured opaque membrane. The prepared phase-inversion membrane was a uniform thickness of about 70–100 μm.

To prepare the evaporation membrane, the obtained casting solution was spread on a glass plate at room temperature under an air atmosphere for 24 h to evaporate the solvent; the membrane was then dried at 40 °C in a vacuum oven for 48 h to eliminate the residual solvent; then a golden-coloured transparent membrane was obtained. The thickness of the evaporation membrane was about 300 μm.

After the membrane preparation process, the as-prepared membranes were immediately immersed in distilled water to remove the solvent of NMP. The membranes were immersed in distilled water for at least a week, and the water was changed three times a day. The residual solvent quantity was detected by an UV-Vis spectrophotometer (UV-1750, Shimadzu Co., Ltd, Japan) at a wavelength of 200 to 500 nm and is shown in ESI Fig. S1† (UV-Vis spectra, before and after one week).

The white opaque membranes prepared *via* the phase inversion method were termed PM-16-0-0, PM-8-8-0, PM-8-6-2, PM-8-4-4, PM-8-2-6 and PM-8-0-8; while the golden-coloured transparent membranes prepared by the evaporation method were termed EM-16-0-0, EM-8-8-0, EM-8-6-2, EM-8-4-4, EM-8-2-6 and EM-8-0-8 (the compositions are shown in Table 1).

2.3.2 Characterization. The membrane surfaces were investigated by ATR-FTIR and X-ray photoelectron spectroscopy (XPS, the take-off angle was 70 degrees). The cross-section morphology of the membranes was observed using a scanning electron microscope (SEM). For observation, the membranes were freeze-dried for 4 h, and then quenched by liquid nitrogen gas, attached to the sample supports and coated with a gold layer. A scanning electron microscope (JSM-7500F, JEOL, Japan) operated at 20 kV accelerating voltage was used to observe the morphology of the membrane cross-section.

The hydrophilicity of the membrane surfaces was characterized based on the static contact angle measurement using a contact angle goniometer (OCA20, Dataphysics, Germany) equipped with a video capture device. A piece of 2 × 2 cm^2 membrane was attached to a glass slide and mounted on the

Table 1 Weight composition of the cast solutions for the prepared phase inversion membranes and evaporation membranes

Membrane type	Membrane no.	PES (wt%)	CEPS (wt%)	SPES (wt%)
Phase-inversion membrane	PM-16-0-0	16	0	0
	PM-8-8-0	8	8	0
	PM-8-6-2	8	6	2
	PM-8-4-4	8	4	4
	PM-8-2-6	8	2	6
	PM-8-0-8	8	0	8
Evaporation membrane	EM-16-0-0	16	0	0
	EM-8-8-0	8	8	0
	EM-8-6-2	8	6	2
	EM-8-4-4	8	4	4
	EM-8-2-6	8	2	6
	EM-8-0-8	8	0	8

goniometer. For the static contact angle measurements, 3 μL double distilled water was dropped on the air-side surface of the membrane at room temperature, and the contact angle was measured after 10 seconds. At least eight measurements were averaged to get a reliable value. The measurement error was ±3°.

2.4 Blood compatibility

All the membranes were treated with phosphate-buffered solutions (PBS, pH = 7.4) before the blood compatibility and cytocompatibility experiments.

2.4.1 Collection of human plasma. Human blood plasma was used to test the blood compatibility of the modified membranes. Whole human fresh blood was collected by venipuncture from a healthy volunteer (man, 25 years old). The blood was mixed with 3.8 wt% anticoagulant citrate dextrose (ACD) (9 : 1, v/v) and centrifuged at 1000 rpm and 4000 rpm for 15 minutes to obtain platelet-rich plasma (PRP) and platelet-poor plasma (PPP), respectively. The plasma was stored at −20 °C until use.[26]

2.4.2 Protein adsorption. For the protein adsorption assay, BFG was dissolved in isotonic PBS (pH = 7.4) with a concentration of 1 mg mL^{-1}. A membrane of 1 × 1 cm^2 area was incubated in the protein solution at 37 °C for 2 h. After protein adsorption, the membrane was slightly rinsed with PBS solution and double distilled water alternately 3 times. The membrane was then immersed in a washing solution (2% sodium dodecyl sulfate, SDS) at 37 °C, and shaken gently for 2 h to remove the protein adsorbed onto the membrane. The amount of the protein eluted in the SDS solution was then quantified usign a Micro BCA™ protein assay reagent kit. The adsorbed protein amount was then calculated. The assays were performed in triplicate for each sample.

2.4.3 Platelet adhesion. Prior to platelet adhesion tests, the membrane (1 × 1 cm^2) was immersed in PBS solution and equilibrated at 37 °C for 1 h. The membrane was then incubated in 1 mL fresh PRP at 37 °C. After 1 h, the PRP was removed with an aspirator, and the membrane was rinsed three times with PBS solution, then the adhering platelets were fixed with 2.5 wt% glutaraldehyde in PBS at 4 °C for 24 h. Finally, the sample was washed with PBS and subjected to a drying process by passing through a series of graded alcohol-PBS solutions (30, 50, 70, 80, 90, 95 and 100%). The critical point when drying the specimens was done with liquid CO_2.[34,35] SEM images were recorded using a scanning electron microscope (JSM-7500F, JEOL, Japan) operated at an accelerating voltage of 20 kV, and the platelet adhesion was investigated. The number of the adhered platelets on the membrane surface was calculated from five SEM pictures at 500× magnification from different places on the same membrane.

2.4.4 Platelet activation. Surface platelet antigen expression was analyzed using immunofluorescence with a flow cytometer (BD FACS calibur). Platelet antigens were detected in the whole blood with anti-$CD62P^{PE}$ (Beckman Coulter, CA) antibodies. The sample was incubated for 15 minutes in the dark at room temperature and was then diluted and fixed with ice-cold PBS containing 1% paraformaldehyde (PFA) to prevent further activation. The method of fixing cells after short incubation with the antibody has been shown not to cause a significant artificial increase in $CD62P^{PE}$ expression due to the fixative treatment.[36] The sample was then analyzed with the Attractor software by acquiring 10 000 platelet events on a FacsCalibur Flow Cytometer (Becton Dickison). Platelets without further treatment and isotypic IgG monoclonal antibodies (Mouse, Bechman Coulter, CA) were used as a negative control and isotype control, respectively.

2.4.5 Clotting time. The anticoagulant activity of the modified membranes was determined using a semi-automatic blood coagulation analyzer (CA-50, Sysmex, Japan) by measuring the clotting times (in seconds) including activated partial thromboplastin time (APTT) and prothrombin time (PT), as follows:[37] the sample membranes (1 × 1 cm^2) were placed carefully in a 24-well cell culture plate. Then 1 mL platelet-poor plasma (PPP) was dropped in each well and then incubated at 37 °C for 0.5 h. Afterwards, 50 μL incubated PPP solution for APTT was warmed in the automated blood coagulation analyzer for 60 seconds and then mixed well with 50 μL of ACTIN (Siemens Healthcare Diagnostics Products GmbH) agent at 37 °C for 3 minutes. Next, the calcium chloride solution (0.025 mol L^{-1}, Dade Behring Marburg GmbH) was added. Finally, the time was obtained by the analyzer. For the PT test, 100 μL incubated PPP solution was warmed in the automated blood coagulation analyzer for 60 seconds and then mixed well with 100 μL of Thromborel® S (Dade Behring Marburg GmbH) agent at 37 °C for 3 minutes, and then the time was obtained. The assays were performed in triplicate for each sample. The difference among individual groups was evaluated using the Student's *t*-test, and the level of significance was chosen as $P < 0.05$.

2.4.6 Coagulation activation and complement activation. Commercial enzyme-linked immunosorbent assays (ELISA) were used to evaluate the coagulation activation (thrombin–antithrombin III complex (TAT), Enzygnost TAT micro, Assay Pro, USA) and complement activation (C3a and C5a, CUSABIO BIOTECH CO., LTD, China). The whole blood incubated for 2 h was centrifuged for 20 minutes at 2000*g* (4 °C) centrifugal force to obtain plasma. Then the plasma was mixed with specific inhibitors for each assay and centrifuged according to the respective instruction manuals. The difference among individual groups was evaluated using the Student's *t*-test, and the level of significance was chosen as $P < 0.05$.

2.5 Cytocompatibility

2.5.1. Cell morphology. For cell morphology observation, hepatocytes were chosen to be seeded onto the membranes at a density of approx. 2.5 × 10^4 cells per cm^2. After 2 days, the seeded membranes were immediately rinsed with PBS and fixed with 2.5% (wt%) glutaraldehyde in PBS at 4 °C for 12 h. The fixed samples were then subjected to a drying process by passing them through a series of graded alcohol-PBS solutions (30, 50, 70, 80, 90, 95 and 100%, 15 minutes for each time) and then dehydrated through isoamyl acetate. The critical

point drying of the specimens was done with liquid CO_2. The specimens were sputter-coated with a gold layer and examined by a SEM (JSM-7500F, JEOL, Japan) operated at an accelerating voltage of 20 kV.

2.5.2 MTT assay. After cell culture for 2, 4 and 6 days, the viability of the hepatocytes was determined using an MTT assay. The hepatocytes were seeded onto the membranes at a density of approx. 2.5×10^4 cells per cm^2. The cells cultured in the wells without the membranes served as the control in this study. After determined time intervals, 45 μL of the MTT solution (1 mg mL^{-1} in the test medium) was added to each well and incubated for 4 h at 37 °C. Mitochondrial dehydrogenases of viable cells selectively cleave the tetrazolium ring, yielding blue/purple formazan crystals. Next, 400 μL of ethanol was added to dissolve the formazan crystals. Therefore, the quantity of the formazan crystals dissolved in the ethanol reflects the level of cell metabolism. The dissolved solution was shaken homogeneously for about 15 minutes using a shaker. The solution of each sample was aspirated into a microtiter plate and the optical density of the formazan solution was read on a Microplate reader (Model 550, Bio-Rad) at 492 nm. All the experiments were repeated three times, and the results were expressed as means ± SD. The statistical significance was assessed using the Tukey–Kramer method, and the level of significance was chosen as $P < 0.05$.

3. Results and discussion

3.1 Characterization of SPES and CPES

Fig. 1(A) shows the ^{1}H-NMR spectra for PES, SPES and CPES. As shown in the spectra, for SPES, a significant chemical shift from δ = 8.0 to δ = 8.3 ppm of the hydrogen located in the *o*-position at the aromatic ring to the sulfone groups is observed, which indicated the sulfonic acid groups have been introduced to the aromatic rings, and the result is consistent with the description in the literature.[32,38] For CPES, the peak at δ = 10.6 is the chemical shift of –COOH, which confirmed that –COOH was introduced onto the PES molecular chain after the oxidation reaction. Moreover, a split of the peak between δ = 7.0 and δ = 8.0 is found, which could also be attributed to the grafted carboxylic groups.

FTIR spectra were also used to confirm the presence of the sulfonic and carboxylic groups of SPES and CPES, respectively. The FTIR spectra of PES, SPES and CPES are shown in Fig. 1(B), and it is found that the spectra of SPES and CPES are different from that of PES. For SPES, the peak at 1025 cm^{-1} could be assigned to the aromatic sulfonic group (–SO_3H) symmetric stretching vibrations and the peak at 3460 cm^{-1} was the characteristic peak of the hydroxyl of the sulfonic groups. For CPES, the peaks at 3440 cm^{-1} and 1772 cm^{-1} indicated the presence of the –OH and –C═O, which should be attributed to the –COOH groups. In summary, the results of ^{1}H NMR and FTIR spectra confirmed that SPES and CPES were successfully synthesized.

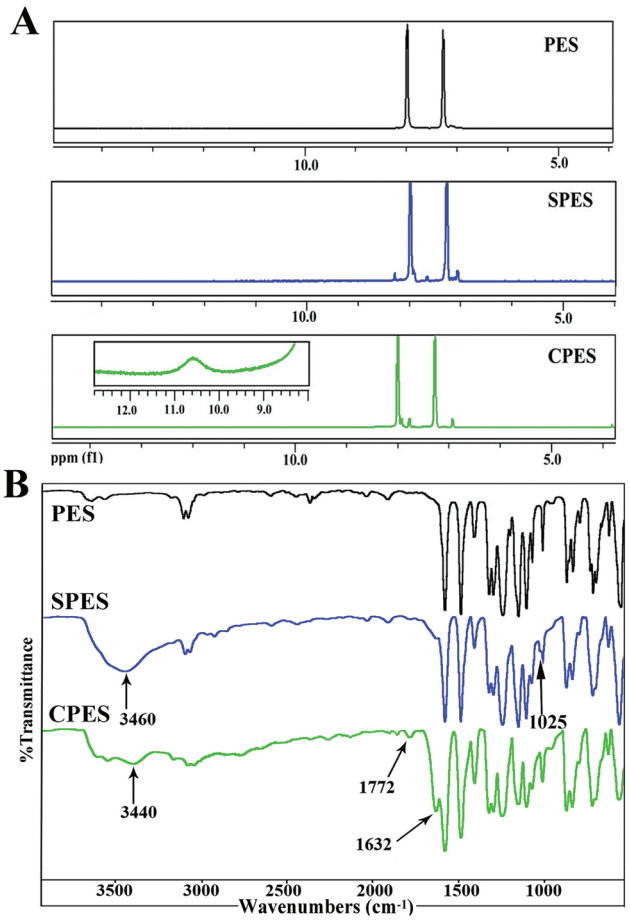

Fig. 1 (A) ^{1}H-NMR spectra of SPES and CPES. For CPES, the inserted figure of chemical shift at 9–12 ppm was obtained by amplifying the baseline; (B) FTIR spectra of SPES and CPES.

3.2 Composition and structure of the modified PES membranes

3.2.1 ATR-FTIR and XPS spectra. Fig. 2 shows the ATR-FTIR spectra of modified membranes prepared *via* evaporation and phase-inversion methods. As shown in the figure, for EM-8-2-6, a peak at 1025 cm^{-1} might be assigned to the stretching vibrations of the aromatic –SO_3H, which belonged to the SPES. In addition, the peak at 1660 cm^{-1} indicates the presence of CPES, and the same phenomenon was found in PM-8-2-6. For the pristine PES membrane, no similar peaks are found. To sum up, the ATR-FTIR spectra demonstrated that sulfonic acid and carboxylic acid groups were introduced to the modified membrane surfaces; and the surface of the modified PES membrane might be regarded as a heparin-like interface with aggregated sulfonic acid and carboxylic acid group enriched polymer chains.

In order to determine the component and composition of the membrane surfaces, the modified membranes were detected by XPS with a take-off angle of 70 degrees. From the data, it can be observed that the contents of element S increase with the SPES increment both for the evaporation and phase-inversion membranes. Compared with the evaporation

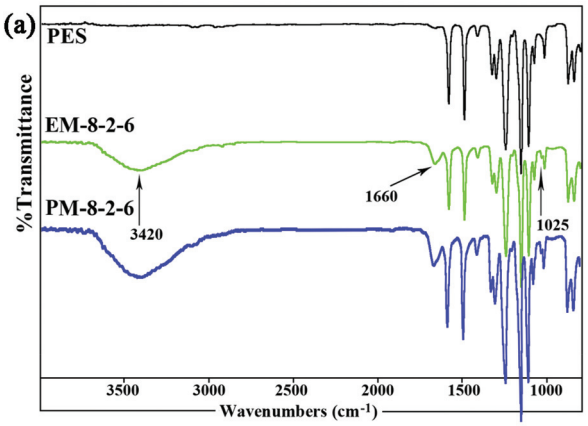

(b)

Samples	C (%)	O (%)	S (%)
PES	73.48	22.13	4.12
EM-8-6-2	62.85	27.03	5.04
EM-8-4-4	62.51	27.55	5.45
EM-8-2-6	62.20	27.62	5.90
PM-8-6-2	62.57	26.91	5.44
PM-8-4-4	62.21	27.45	5.85
PM-8-2-6	61.90	27.49	6.33

Fig. 2 (a) FTIR spectra of the PES and the modified PES membranes; (b) the contents of the elements C, O, and S in the modified membranes detected by XPS (mass fraction).

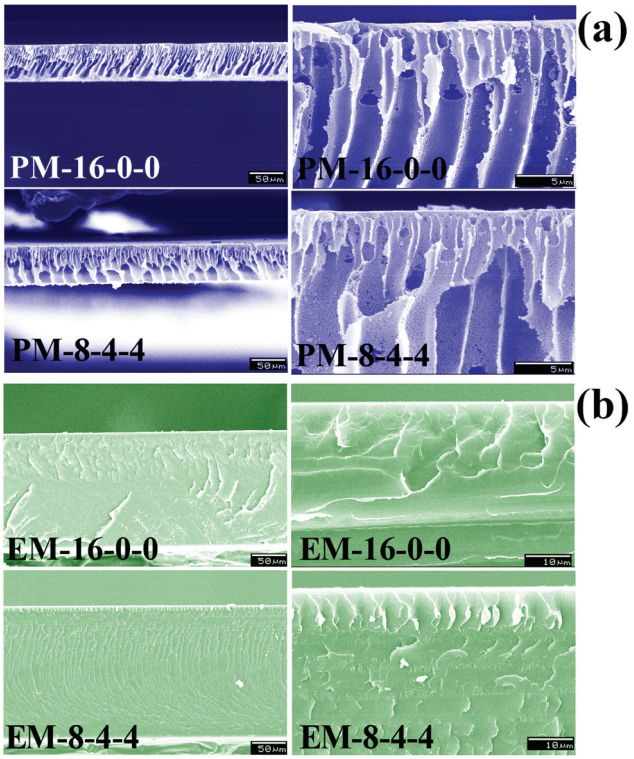

Fig. 3 Cross-section views for PES and modified PES membranes. (a) For the phase-inversion membrane, blue colour images, the scale bar is 50 μm (left) and 5 μm (right); (b) for the evaporation membrane, green colour images, the scale bar is 50 μm (left) and 10 μm (right).

membrane, the contents of element S in the phase-inversion membranes are lower, since surface aggregation of SPES and CPES could occur more intensively in the phase-inversion membrane during the membrane preparation procedure. From the ATR-FTIR and XPS results, it could be demonstrated that the CPES and SPES were successfully immobilized on the modified membrane surface in an appropriate ratio.

3.2.2 SEM pictures. Fig. 3 shows the cross-section SEM micrographs for the membranes. For the phase-inversion membrane (Fig. 3(a)), the characteristic morphology of the asymmetric membrane consisting of a dense top-layer and porous sub-layer with a finger-like structure is observed. For the modified membrane, the pore diameter of the finger-like structure is larger, and the porous sub-layer is less erratic and obvious compared to that of the PES membrane. For the evaporation membrane (Fig. 3(a)), it is found that the membrane consists of two parts: (i) the top layer with a thickness of 15 μm made of relatively oriented fibrous components, and (ii) the bottom layer with an irregular morphology. The fibrous component of the modified membrane is more oriented compared with that of the pristine PES membrane. Solvent evaporation on the glass surface provides a relatively homogeneous membrane, which is made of the fibrous component. The precise mechanism of the structure formation during the evaporation process is still not clear, but the results showed that the structure of the PES membrane was changed by the addition of SPES and CPES. The SEM structure results suggested that the cross-sectional structures of the membranes had been altered, at least in part, with the blending of SPES and CPES.

3.3 Water contact angles (WCA)

Fig. 4 shows the WCAs for both the phase-inversion and evaporation membranes. It is observed that the water contact angle decreased with the addition of CPES in the membranes. The addition of SPES further decreased the WCA. Higuchi[39] and Nakagawa[40] pointed out that a material with $-CH_2SO_3-$

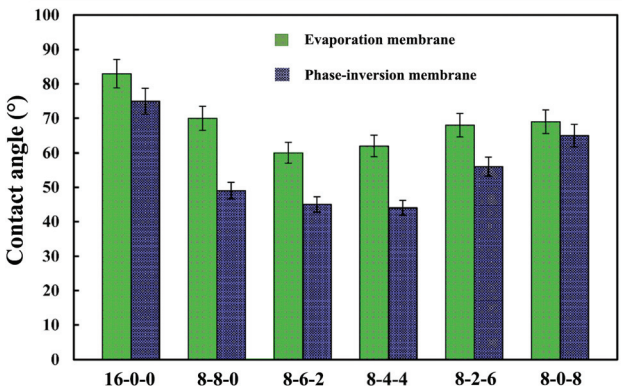

Fig. 4 The water contact angles of the membranes (phase-inversion membrane and evaporation membrane). The results are expressed as means ± SD (n = 8).

segments had better hydrophilic property. Moreover, from this figure, it is found that the WCAs of the phase-inversion membranes decreased significantly compared to those of the evaporation membranes. This fact might be explained by the results that the surface morphology of the evaporation membrane were much more different from those of the phase-inversion membrane due to the different driving forces and different solvent migration times during the membrane preparation process. More detailed work is needed to explore the different effect of phase-inversion and evaporation membranes on the WCAs. In general, the decreased WCAs of the modified membranes indicate that the blending of SPES and CPES could enhance the hydrophilic property of the PES membrane surface.

3.4 Blood compatibility

3.4.1 Protein adsorption. Adsorption of plasma protein occurs on the surface as soon as blood is in contact with a biomaterial, following this are platelet adhesion and activation of coagulation pathways, leading to thrombus formation.[41] Thus, recent studies suggested that the amount of protein adsorbed on the membrane material was one of the most essential factors in evaluating the blood compatibility of materials.[42,43] There are many factors that affect the interaction between membrane surface and protein, such as surface charge character, surface free energy and topological structure, solution environment (*e.g.* pH, ionic strength), and protein characteristics.[44,45] In this study, protein adsorption on the modified membrane surface was evaluated in relation to the adsorption of bovine fibrinogen (BFG) *in vitro*.

Fig. 5 shows the adsorption results of BFG on the membrane surface from PBS solutions (1 mg mL^{-1}). As shown in the figure, it is found that the amounts of adsorbed BFG decreases with the addition of CPES for the two kinds of membranes, and further decreases with blending SPES, attributed to the synergistic influence of the CPES and SPES additives. The reduced BFG adsorption was in good agreement with the increased hydrophilicity of the membrane surfaces. The hydrophilic/hydrophobic character of the membrane material played a relatively important role in the interaction between protein and membrane. Since the hydrophilic surface preferentially adsorbed water rather than solutes, many researchers had followed the idea of increasing the hydrophilicity of a membrane material with the goal of reducing protein fouling and/or protein adsorption.[46] In this study, the CPES and SPES contained hydrophilic functional groups, which endowed the modified membrane surfaces with high hydrophilicity. Han *et al.*[47] suggested that negatively charged sulfonate groups exhibited relative low BFG adsorption amounts. Furthermore, with the synergistic effect of the sulfonic acid and carboxylic acid groups, the BFG adsorption of the PES/CPES/SPES was lower than that on the pristine PES membrane. The hydrophilicity and the negatively charged groups of the membrane surfaces should be responsible for the decrease of the protein adsorption.

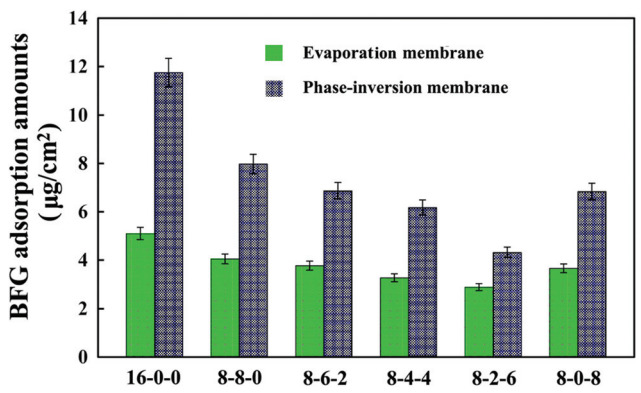

Fig. 5 Bovine serum fibrinogen (BFG) adsorption amounts onto the membranes. The results are expressed as means ± SD (n = 3).

In addition, it could be observed that the adsorbed BFG amounts on the phase-inversion membranes were higher compared with those on the evaporation membranes. The results could be attributed to the different surface morphologies of the phase-inversion and evaporation membranes which were formed during the phase-inversion and evaporation process, respectively. Furthermore, the two types of modified membrane exhibited the lowest amount of BFG adsorption when the ratio of SPES to CPES was 6 : 2. These results indicate that the BFG adsorption could be visibly decreased due to the CPES and SPES, which provided carboxylic and sulfonic groups, respectively. The decreased protein adsorption was caused by these functional groups, which might improve the blood compatibility of the membranes; and the modified membranes might exhibit a heparin-like anticoagulant activity,[48] which will be discussed in the following sections.

3.4.2 Platelet adhesion. The extent of platelet adhesion and platelet aggregation is considered to be a crucial step in the process of thrombus formation. After platelet adhesion, a series of actions could produce thrombin formation, and led to further coagulation. Thus, in this study, the morphology of the adherent platelets and the adhered platelet number was investigated.

Fig. 6(a) shows the SEM micrographs of the platelets adhering onto the evaporated PES and modified PES membranes. As shown in the figure, with the same amplification multiple, it is observed that on the pristine PES membrane surface, numerous platelets are adhered and aggregated. Platelet aggregation on the pristine PES membrane indicated that thrombus formation might occur at the surface of the membrane, which is a life-threatening phenomenon for patients. However, for the modified membranes, very few platelets are found; and the platelets express a rounded morphology with nearly no pseudopodium and deformation. Fig. 6(b) shows the numbers of the platelet clusters adhered on the phase-inversion membranes from platelet-rich plasma. The modified membranes show a much lower number of adhered platelets compared with that of the PES membrane. From these figures, it could be observed that the platelet adhesion was distinctly decreased, and most platelets retained their discoid shape on the modified membranes. As the ratio of CPES to SPES varied,

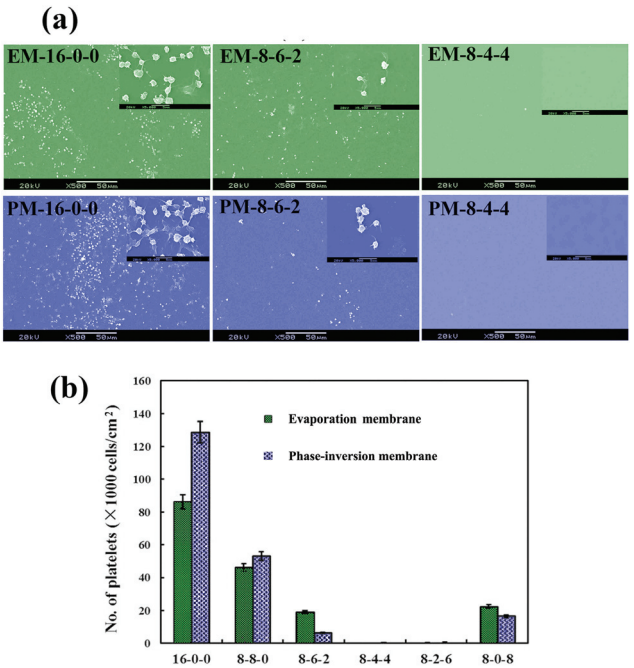

Fig. 6 (a) Scanning electron micrographs of the adherent platelets onto the membranes; (b) number of adhered platelets on the membranes.

the adhering platelet number changed; remarkably, barely any adhered platelet was found on the surface of the M-8-4-4. The platelet adhesion results were consistent with the previous BFG adsorption. Fibrinogen was a known mediator for platelet adhesion and aggregation.[49] The reduced platelet adhesion should be attributed to the surface introduction of the sulfonic and carboxylic groups of the modified membrane and the resulting decrease in BFG adsorption. Therefore, based on the platelet adhesion results, the modified membranes might have improved blood compatibility.

3.4.3 Platelet activation. Platelet activation is a common phenomenon when a membrane contacts with blood. Flow cytometry technology could be applied for the measurement of platelet activation at the level of the platelet positive expression of CD62p. In this study, we examined platelet activation using the percentage of CD62p expression on the platelets.

The results of platelet activation showed a slight increase in the percentages of CD62p-positive PLTs for both phase-inversion and evaporation membranes compared with the control sample. For the 8-4-4 membranes, the percentages of CD62p-positive PLTs showed no difference from that of the negative control (ESI Fig. S2†). The results indicated that the activation of platelets for the modified membranes with both sulfonic and carboxylic groups was significantly decreased compared to the pure PES membrane, and that the heparin-like structure of the surface could decrease platelet activation due to the functional groups.

3.4.4 Clotting time. There are three pathways in the blood coagulant system, including the intrinsic pathway, the extrinsic pathway, and the common pathway. In this study, APTT and PT were used to evaluate mainly the intrinsic and extrinsic pathways.[14] Fig. 7 shows APTT and PT test results for the membranes. From Fig. 7(a), it is found that the clotting times for the modified membranes prepared by both phase inversion and evaporation methods were significantly prolonged compared with that of the pristine PES membrane ($P < 0.05$). The 8-2-6 modified membranes show clotting times approximately twice as long as APTT compared with the pure PES membrane ($P < 0.05$). Meanwhile, the same phenomenon could be found in the PT results, although its increment range was lower than APTT (Fig. 7(b)). These results suggested that the sulfonic and carboxylic groups might be effective groups in prolonging the blood clotting time. In addition, the improvement of anticoagulant activity was in good agreement with the increased hydrophilicity, decreased protein adsorption, and suppressed platelet adhesion and activation.

Comparing Fig. 7(a) and (b), for most of membranes it is obvious that the APTT and PT of the modified membranes prepared by the phase inversion method were longer than those prepared by the evaporation method, with an increase of about 10 seconds. This might be due to the different formation processes for evaporation and phase-inversion membranes, which led to different surface morphology. Moreover, the results could also be attributed to the surface aggregation amounts of the SPES and CPES.[50]

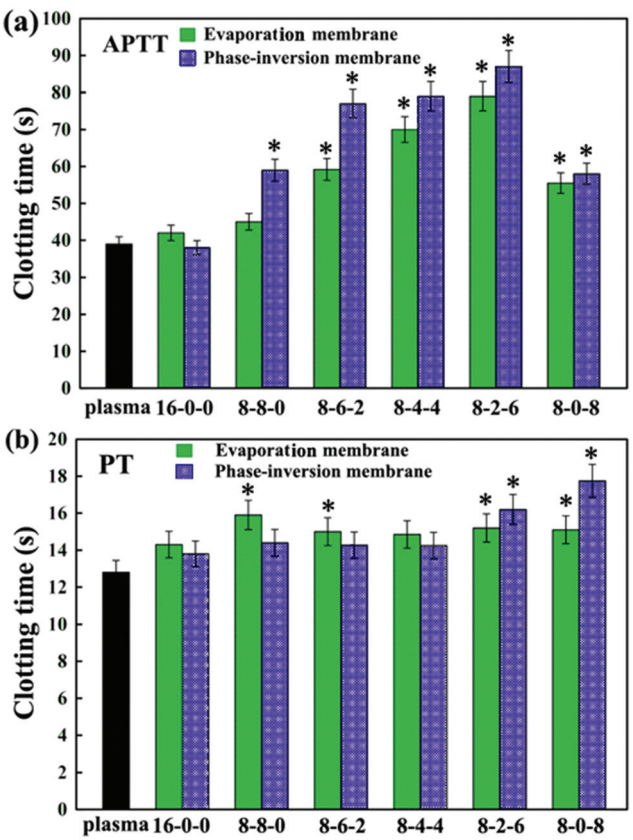

Fig. 7 (a) APTT, and (b) PT assays for the PES and modified PES membranes. The results are expressed as means ± SD ($n = 3$), *$P < 0.05$ compared to the values of the 16-0-0 membrane (APTT and PT).

3.4.5 Coagulation activation. When blood is in contact with a material surface, thrombin activity is generated. Quantification of thrombin generation by the unphysiologic surface is a major challenge for the hemostasis laboratory, and thrombin generation assays are also very essential. The amount of generated thrombin is evaluated through measurement of the amount of thrombin–antithrombin III (TAT), since the thrombin would be immediately inactivated when reacted with antithrombin-III, resulting in the formation of a TAT complex. Hence, the compatibility of the modified membranes with coagulation system was investigated in terms of TAT generation.

Fig. 8 shows the thrombin–antithrombin III (TAT) generation results of the membranes. Compared with the control sample, no significant increase is observed in the values of the TAT generation amounts for the PES-based membranes, which suggested that the TAT generation was not affected by the addition of the SPES and CPES. The results suggested that no obvious activation of the coagulation cascade occurred after the modified PES membranes contacting with blood, and the modified PES membranes had good blood compatibility.

In addition, the phase-inversion membranes showed slightly decreased TAT generation compared with the evaporation membranes. This was in good accordance with the results of platelet adhesion and anticoagulant activity assay. This could also be explained by the different formation processes.

Thus, it could be concluded that phase inversion method modified membrane had great potential to approach the highly blood compatible membranes, and this study provided enlightening information for the design of a modified membrane using phase-inversion and evaporation.

3.4.6 Complement activation. Complement activation is the triggering of the host defence mechanism generated by the localized inflammatory mediator. Hemodialysis membranes show activation of complement through an alternative pathway. Complement activation could be measured by determining the generated anaphylatoxins C3a, C4a and C5a. In this study, C3a and C5a concentrations were determined using an ELISA assay for complement activation evaluation.

The concentrations of C3a and C5a are used to evaluate the complement activation, and the results are presented in Fig. 9. As shown in Fig. 9(a), by blending SPES and CPES in the membranes, the activated C3a concentrations decreased compared with that of the pristine PES membrane, especially for the phase inversion membranes. Moreover, the membranes (PM-8-6-2, PM-8-4-4, and PM-8-2-6) prepared by the phase inversion method showed significantly decreased concentrations of complement fragment C3a compared with the control sample. However, the membranes (EM-8-6-2, EM-8-4-4, and EM-8-2-6) prepared by the evaporation process showed no obvious difference when compared with the control sample at the C3a level. These results demonstrate that the PES/CPES/SPES membranes successfully inhibited the formation of soluble C3a in blood plasma compared with the PES membrane.

Similar results are observed for the C5a concentrations (Fig. 9(b)). No significant difference in C5a levels is observed for the modified membranes compared to the control sample, except that the pristine PES membrane prepared by evaporation method showed a significant increase in C5a level.

Some researchers pointed out that the surface contact activation usually occurred when blood-contacting materials

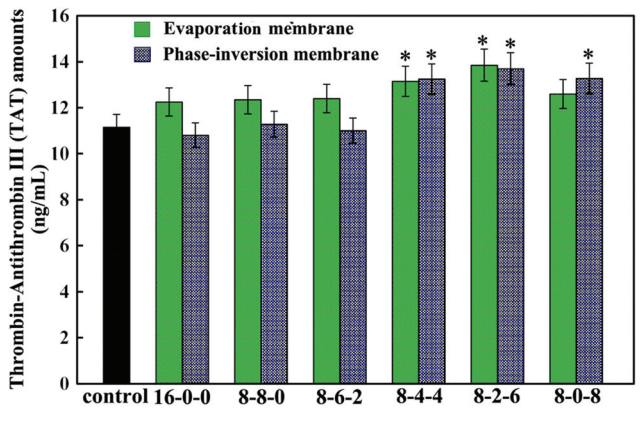

Fig. 8 The thrombin–antithrombin III (TAT) generation of the membranes with PRP flowing for 2 h. The results are expressed as means ± SD (n = 3), *P < 0.05 compared to the value of the 16-0-0 membrane.

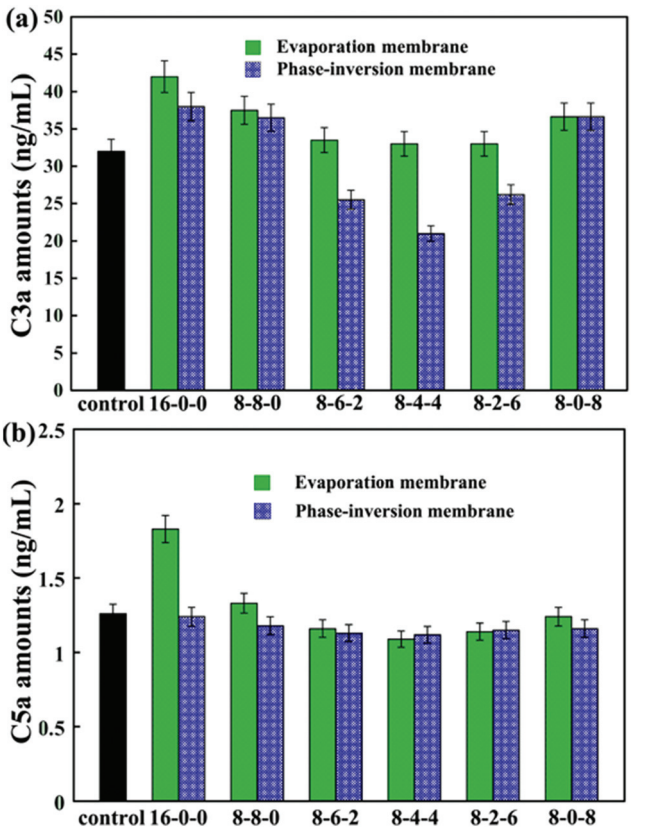

Fig. 9 (a) The concentrations of C3a for the samples with whole blood incubated for 2 h. The results were expressed as means ± SD (n = 3); (b) the concentrations of C5a for the samples with whole blood incubated for 2 h. The results are expressed as means ± SD (n = 3).

contacted with blood, especially negatively charged surfaces, which then led to the activation of the coagulation cascade.[51,52] This activation of the coagulation cascade could result in the formation of thrombin and fibrin clots.[53] Simultaneously, the formed thrombin and fibrin could activate platelets and promote the formation of a thrombus. In this study, in order to mimic the heparin-like surface, –COOH and $–SO_3H$ groups (negatively charged groups) were introduced to the modified PES membrane surface. From the results of CD62p-positive platelets expression and TAT complex amounts, it could be found that no significant evidence for contact phase activation occurred, especially in the modified membranes PM-8-4-4 and EM-8-4-4. Thus, the contact phase activation could be controlled by regulating the –COOH and $–SO_3H$ density in an appropriate range. Moreover, from the results of the blood compatibility test, it could be observed that when we introduced both –COOH and $–SO_3H$, the blood compatibility of the modified membranes was better than that of the modified membrane that only had –COOH or $–SO_3H$ introduced. Therefore, it could be speculated that a synergistic effect of –COOH and $–SO_3H$ at the modified membrane surface might occur when contacting with blood.

In general, inspired by the chemical structure of heparin molecules, we have successfully modified a PES membrane surface with a heparin-like interface *via* a blending method, as shown in Fig. S3.† Both SPES and CPES can be directly blended with PES in any proportion to form miscible polymer blends due to their similar molecular backbones. The modified membrane showed better hydrophilicity, decreased protein adsorption, suppressed platelet adhesion, suppressed platelet activation, reduced TAT generation, prolonged APTT, and limited activation of C3a and C5a compared to the pure PES membrane. Most importantly, the platelet activation and thrombin generation results suggested that nearly no contact activation occurred after the blood contacted with the modified PES membrane surface, which indicated that the modified membranes might possess intrinsic blood compatibility and could satisfy various blood contacting applications.

3.5 Bio-artificial liver related cell proliferation

As the PES membranes were expected to be used as biomaterials in bio-artificial liver supports, bio-artificial liver related cell proliferation also played a critical role for the modified membranes. Thus, cell proliferation of the modified membranes was evaluated in terms of cell morphology and cytotoxicity. Human hepatocytes LO2 were chosen for the cell culture experiments.

3.5.1 Cell morphology analysis. The morphology of hepatocyte cells were observed using SEM at different amplification multiples. As shown in Fig. 10, hepatocyte cells adhered to the membranes, and spread in pseudopodia to form cell layers on the surface. Fig. 10(a) indicates that the morphology of hepatocytes cultured on the modified membrane (PM-8-4-4) was generally similar to that of the hepatocytes seeded on the pure PES membrane (PM-16-0-0), SPES modified membrane (PM-8-8-0) and CPES modified membrane (PM-8-0-8).

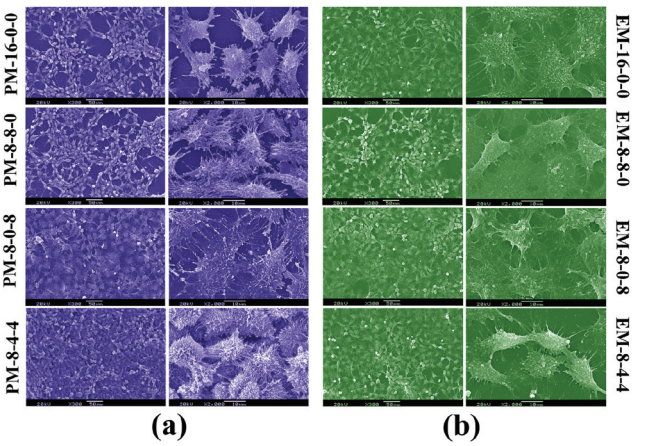

Fig. 10 SEM pictures of human hepatocytes LO2 cultured on the membranes for 2 days: (a) hepatocytes on phase-inversion membranes; (b) hepatocytes on evaporation membranes.

However, it was observed that the amounts of the hepatocytes on the modified membrane gradually increased with the introduction of SPES and CPES compared with that of the PES membrane. Moreover, the membrane surface of PM-8-4-4 was fully covered by the cells which were gathered together with the extending pseudopodia. The morphology of the hepatocytes cultured on the modified membranes indicated a better cell spread and cell proliferation, which implied that the modified membrane did promote the growth of hepatocytes, and maintained better cytocompatibility compared with the PES membrane. Furthermore, from Fig. 10(b), it is found that the hepatocytes displayed spindle morphology on the surface of the evaporation membranes, and no significant difference was found among these images. These results suggested that the cell proliferation of the modified membranes through the evaporation method might not be obviously improved due to the smooth surface structure. An MTT test was subsequently assayed on the hepatocyte cultivated membranes (Fig. 11) and the hepatocytes cultured on a blank plate were set as the control sample for further comparison.

3.5.2 MTT assay. Fig. 11 shows the MTT results for the negative control and the membranes, the results were analyzed using statistical methods (statistical significance using the Tukey–Kramer multiple comparison, $P < 0.05$).[54,55] The formazan absorbance implied that the succinate dehydrogenase in the mitochondria of living cells was able to convert exogenous MTT reduction into a water-insoluble crystalline blue formazan product that deposited on the cells, which could dissolve in ethanol; this could not happen in dead cells. As shown in Fig. 11, the absorbance for all the membranes increased with an increase of culture time. However, for the phase inversion membrane (Fig. 11(a)), on the second day, fourth day and sixth day, the viability of the hepatocytes on the membranes with the addition of both CPES and SPES increased compared with those on pristine PES membrane (PM-16-0-0) and PM-8-0-8 membrane ($^*P < 0.05$); moreover, the modified PES membranes with both CPES and SPES kept a better viability during

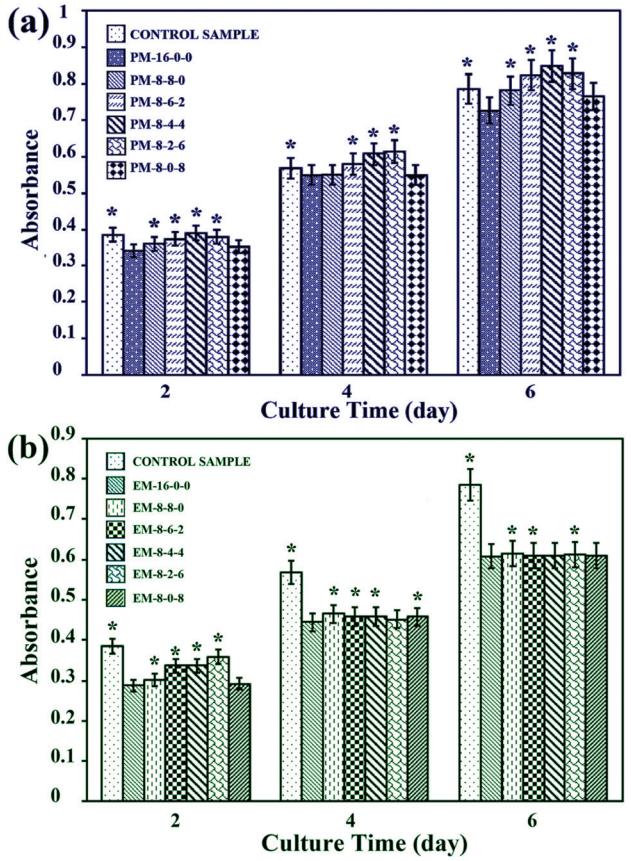

Fig. 11 MTT-tetrazolium assays. Formazan absorbance expressed as a function of time from hepatocytes seeded onto different membranes and the controls: (a) formazan absorbance for phase inversion membranes; (b) formazan absorbance for evaporation membranes. The results are expressed as means ± SD (n = 3), *P < 0.05 compared to the values of PM-16-0-0 and EM-16-0-0 membranes for 2, 4 and 6 days.

the whole culture time, which suggested that the introduction of both sulfonic acid and carboxylic acid groups might have a positive effect on the cytocompatibility of the membranes. On the other hand, from Fig. 11(b), it is observed that the viability of the hepatocytes for all the evaporation membranes showed nearly no difference with culture time (*P < 0.05), which was in good agreement with the cell morphology results. Based on these data, we inferred that the evaporation method for preparing the membrane might have no significant influence on the improvement of cytocompatibility and cell proliferation for the membranes.

Therefore, it could be concluded that better cell proliferation could be obtained with the addition of both CPES and SPES into PES membranes, and the modified membranes prepared by the phase inversion method have potential to be used for bio-artificial liver supports.

4. Conclusions

Inspired by the chemical structure of heparin molecules, we have successfully modified a PES membrane surface with a heparin-like interface *via* a blending method with enhanced biocompatibility. Clinical complications associated with current hemodialysis PES membranes might be improved using the SPES and CPES as additives. Both SPES and CPES can be directly blended with the PES matrix in any proportion to form miscible polymer blends due to their similar molecular chains, and can be prepared into evaporation and phase-inversion membranes. The SPES and CPES had a synergistic effect on the improvement of the modified membranes, and these obtained PES/CPES/SPES membranes showed better hydrophilicity, decreased protein adsorption, suppressed platelet adhesion and activation, reduced TAT generation, prolonged APTT, and limited activation of C3a and C5a compared to the pure PES membrane. The modified membranes prepared *via* phase inversion proved to be better than those prepared by the evaporation method in terms of blood compatibility performance. Furthermore, the platelet activation and thrombin generation results suggested that nearly no contact activation occurred after blood contacting with the modified PES membrane surface. Thus, the modified membrane prepared by the phase inversion technique has great potential in applications for blood purification, including hemodialysis and bio-artificial liver support. Moreover, this study provided useful information for the industrial and clinical application of the membranes. The significance of enhanced blood and cell compatibility of the modified PES membranes with a heparin-like surface prepared by the phase inversion method as described here is not restricted to PES membranes, but may enlighten the modification of some other blood-contacting materials in general.

Acknowledgements

This work was financially sponsored by the National Natural Science Foundation of China (no. 51073105, 51173119, and 51225303), and the Program for Changjiang Scholars and Innovative Research Team in the University (IRT1163). We should also thank our laboratory members for their generous help, and gratefully acknowledge the help of Ms H. Wang, of the Analytical and Testing Center at Sichuan University, for the SEM, and Ms Liang, of the Department of Nephrology at West China Hospital, for the fresh human blood collection.

Notes and references

1 C. Mao, Y. Qiu, H. Sang, H. Mei, A. Zhu, J. Shen and S. Lin, *Adv. Colloid Interface Sci.*, 2004, **110**, 5–17.
2 C. Cheng, S. Nie, S. Li, H. Peng, H. Yang, L. Ma, S. Sun and C. Zhao, *J. Mater. Chem. B*, 2013, **1**, 265–275.
3 M. Ulbricht, O. Schuster, W. Ansorge, M. Ruetering and P. Steiger, *Sep. Purif. Technol.*, 2007, **57**, 63–73.
4 S. David, D. Gerra, C. De Nitti, B. Bussolati, U. Teatini, G. R. Longhena, C. Guastoni, N. Bellotti, F. Combarnous and C. Tetta, Polyethersulfone: Membranes for Multiple

Clinical Applications, *Contrib. Nephrol.*, Basel, Karger, 2003, 138, 43–54.
5 C. S. Zhao, T. Liu, Z. P. Lu, L. P. Chen and J. Huang, *Artif. Organs*, 2001, **25**, 60–63.
6 R. H. Tullis, R. P. Duffin, M. Zech and J. L. Ambrus, *Ther. Apher.*, 2002, **6**, 213–220.
7 C. Sperling, M. Houska, E. Brynda, U. Streller and C. Werner, *J. Biomed. Mater. Res., Part A*, 2006, **76**, 681–689.
8 J. H. Kim and C. K. Kim, *J. Membr. Sci.*, 2005, **262**, 60–68.
9 Z. B. Liu, X. P. Deng, M. Wang, J. X. Chen, A. M. Zhang, Z. W. Gu and C. S. Zhao, *J. Biomater. Sci., Polym. Ed.*, 2009, **20**, 377–397.
10 C. Cheng, S. Li, W. F. Zhao, Q. Wei, S. Q. Nie, S. D. Sun and C. S. Zhao, *J. Membr. Sci.*, 2012, **417**, 228–236.
11 B. H. Fang, Q. Y. Ling, W. F. Zhao, Y. L. Ma, P. L. Bai, Q. Wei, H. F. Li and C. S. Zhao, *J. Membr. Sci.*, 2009, **329**, 46–55.
12 C. S. Zhao, J. M. Xue, F. Ran and S. D. Sun, *Prog. Mater. Sci.*, 2013, **58**, 76–150.
13 K. Ishihara, K. Fukumoto, Y. Iwasaki and N. Nakabayashi, *Biomaterials*, 1999, **20**, 1545–1551.
14 K. Ishihara, K. Fukumoto, Y. Iwasaki and N. Nakabayashi, *Biomaterials*, 1999, **20**, 1553–1559.
15 T. Hasegawa, Y. Iwasaki and K. Ishihara, *Biomaterials*, 2001, **22**, 243–251.
16 L. P. Zhu, Z. Yi, F. Liu, X. Z. Wei, B. K. Zhu and Y. Y. Xu, *Eur. Polym. J.*, 2008, **44**, 1907–1914.
17 M. Ulbricht, H. Matuschewski, A. Oechel and H. G. Hicke, *J. Membr. Sci.*, 1996, **115**, 31–47.
18 H. Susanto and M. Ulbricht, *Langmuir*, 2007, **23**, 7818–7830.
19 H. Engelberg, *Pharmacol. Rev.*, 1996, **48**, 327–352.
20 M. Fukutomi, S. Kobayashi, K. Niwaya, Y. Hamada and S. Kitamura, *Artif. Organs*, 1996, **20**, 767–776.
21 S. Svenmarker, E. Sandstrom, T. Karlsson, E. Jansson, S. Haggmark, R. Lindholm, M. Appelblad and T. Aberg, *Eur. J. Cardiothorac. Surg.*, 1997, **11**, 957–964.
22 D. Labarre, *Int. J. Artif. Organs*, 1990, **13**, 651.
23 P. Joshi, K. F. Schilke, A. Fry, J. McGuire and K. Bird, *Int. J. Biol. Macromol.*, 2010, **47**, 98–103.
24 D. S. Wavhal and E. R. Fisher, *J. Membr. Sci.*, 2002, **209**, 255–269.
25 G. M. Bernacca, M. J. Gulbransen, R. Wilkinson and D. J. Wheatley, *Biomaterials*, 1998, **19**, 1151–1165.
26 C. Cheng, S. Li, S. Nie, W. Zhao, H. Yang, S. Sun and C. Zhao, *Biomacromolecules*, 2012, **13**, 4236–4246.
27 F. Ran, S. Nie, J. Li, B. Su, S. Sun and C. Zhao, *Macromol. Biosci.*, 2012, **12**, 116–125.
28 M. Tang, J. M. Xue, K. L. Yan, T. Xiang, S. D. Sun and C. S. Zhao, *J. Colloid Interface Sci.*, 2012, **386**, 428–440.
29 S. Q. Nie, J. M. Xue, Y. Lu, Y. Q. Liu, D. S. Wang, S. D. Sun, F. Ran and C. S. Zhao, *Colloids Surf., B*, 2012, **100**, 116–125.
30 L. L. Li, C. Cheng, T. Xiang, M. Tang, W. F. Zhao, S. D. Sun and C. S. Zhao, *J. Membr. Sci.*, 2012, **405**, 261–274.
31 R. Guan, H. Zou, D. P. Lu, C. L. Gong and Y. F. Liu, *Eur. Polym. J.*, 2005, **41**, 1554–1560.
32 I. C. Kim, J. G. Choi and T. M. Tak, *J. Appl. Polym. Sci.*, 1999, **74**, 2046–2055.
33 D. Wang, W. Zou, L. Li, Q. Wei, S. Sun and C. Zhao, *J. Membr. Sci.*, 2011, **374**, 93–101.
34 G. M. R. Wetzels and L. H. Koole, *Biomaterials*, 1999, **20**, 1879–1887.
35 A. Higuchi, K. Shirano, M. Harashima, B. O. Yoon, M. Hara, M. Hattori and K. Imamura, *Biomaterials*, 2002, **23**, 2659–2666.
36 V. Schmidt, T. Hilberg, G. Franke, D. Gläser and H. H. W. Gabriel, *Platelets*, 2003, **14**, 287–294.
37 W. C. Lin, D. G. Yu and M. C. Yang, *Colloids Surf., B.*, 2005, **44**, 82–92.
38 I. S. Byun, I. C. Kim and J. W. Seo, *J. Appl. Polym. Sci.*, 2000, **76**, 787–798.
39 A. Higuchi, N. Iwata and T. Nakagawa, *J. Appl. Polym. Sci.*, 1990, **40**, 709–717.
40 A. Higuchi and T. Nakagawa, *J. Appl. Polym. Sci.*, 1990, **41**, 1973–1979.
41 J. D. Andrade and V. Hlady, *Ann. N. Y. Acad. Sci.*, 1987, **516**, 158–172.
42 W. B. Tsai, J. M. Grunkemeier, C. D. McFarland and T. A. Horbett, *J. Biomed. Mater. Res.*, 2002, **60**, 348–359.
43 W. B. Tsai, Q. Shi, J. M. Grunkemeier, C. McFarland and T. A. Horbett, *J. Biomater. Sci., Polym. Ed.*, 2004, **15**, 817–840.
44 Y. X. Leng, J. Y. Chen, P. Yang, H. Sun, G. J. Wan and N. Huang, *Surf. Sci.*, 2003, **531**, 177–184.
45 T. I. T. Okpalugo, A. A. Ogwu, P. D. Maguire and J. A. D. McLaughlin, *Biomaterials*, 2004, **25**, 239–245.
46 D. Mockel, E. Staude and M. D. Guiver, *J. Membr. Sci.*, 1999, **158**, 63–75.
47 D. K. Han, K. D. Park, G. H. Ryu, U. Y. Kim, B. G. Min and Y. H. Kim, *J. Biomed. Mater. Res.*, 1996, **30**, 23–30.
48 D. K. Han, N. Y. Lee, K. D. Park, Y. H. Kim, H. I. Cho and B. G. Min, *Biomaterials*, 1995, **16**, 467–471.
49 A. L. Bailly, A. Laurent, H. Lu, I. Elalami, P. Jacob, O. Mundler, J. J. Merland, A. Lautier, J. Soria and C. Soria, *J. Biomed. Mater. Res.*, 1996, **30**, 101–108.
50 F. Ran, S. Nie, W. Zhao, J. Li, B. Su, S. Sun and C. Zhao, *Acta Biomater.*, 2011, **7**, 3370–3381.
51 G. J. Miller, J. K. Cruickshank, L. J. Ellis, R. L. Thompson, H. C. Wilkes, Y. Stirling, K. A. Mitropoulos, J. V. Allison, T. E. Fox and A. O. Walker, *Atherosclerosis*, 1989, **78**, 19–24.
52 J. M. Nigretto, E. Corretge and M. Jozefowicz, *Biomaterials*, 1989, **10**, 449–454.
53 M. B. Gorbet and M. V. Sefton, *Biomaterials*, 2004, **25**, 5681–5703.
54 H. Nazar, P. Caliceti, B. Carpenter, A. I. El-Mallah, D. G. Fatouros, M. Roldo, S. M. van der Merwe and J. Tsibouklis, *Biomater. Sci.*, 2013, **1**, 306–314.
55 F. R. Rose, L. A. Cyster, D. M. Grant, C. A. Scotchford, S. M. Howdle and K. M. Shakesheff, *Biomaterials*, 2004, **25**, 5507–5514.